Experimental Study and Simulation of the Polymerization of Methyl Methacrylate at High Temperature in a Continuous Reactor

F. FENOUILLOT,* J. TERRISSE , T. RIMLINGER

ECPM, Laboratoire des Procédés et Matériaux Polymères, 25 rue Becquerel, F67087 Strasbourg Cedex 2, France

Received 19 November 1999; accepted 1 June 2000

ABSTRACT: The bulk polymerization of MMA at high temperature (120–180°C) in a continuous pilot-plant reactor has been studied. The polymerization is initiated by diterbutyle peroxide and the chain transfer agent is 1-butanethiol. A simulation program has been developed to predict the steady state behavior of the reactor. The particular features of the kinetic at above-T_g temperature are included in the model, especially the thermal initiation of the reation and the attenuation of the autoacceleration effect. For the flow and mixing model, the actual vessel cannot be approximated to a single ideal reactor because of its design and of the moderate agitation imposed by the high viscosity of the reacting fluid. A tanks in series model with a recycle stream between tanks is proposed to evaluate the backmixing caused by the special design of the agitator. The parameters of the model are determined with the help of the experimental residence time distribution measured on the reactor. The data collected on the actual reactor, i.e., operation, conversion, molecular weight, temperature, are compared to the calculated one. The agreement is satisfactory but the tendencies are slightly underestimated. The program is a tool to evaluate the effect of modifications of the design of the reactor or changes on the operation parameters like input rate, temperature, and agitation on its behavior. © 2001 John Wiley & Sons, Inc. J Appl Polym Sci 79: 2038–2051, 2001

Key words: methyl methacrylate; high temperature; continuous reactor; simulation

INTRODUCTION

The polymerization of methyl methacrylate (MMA) has been studied a lot since the 1960s. One reason is the fundamental scientific interest to acquire a better understanding of the radical polymerization and especially of the strong autoacceleration effect existing for MMA. The other reason, linked to the previous one, is that this gel effect is one of the causes of the difficulties encountered in polymerizing industrially the MMA. Growing from the monomer to a high molecular weight polymer, the viscosity of the reacting medium levels up of about 6 orders of magnitude in the absence of solvent. This viscosity increase is accompanied by a strong heat generation caused by the exothermal nature of the reaction (58×10^3 J/mole would cause a temperature raise of 380°C if the reaction was done under adiabatic conditions). The temperature and viscosity raise may lead to uncontrollable or at least unstable process with the ultimate risk of plugging of the reactor. In addition, a poor quality polymer may

Correspondence to: F. Fenouillot (Francoise.Fenouillot@insa-lyon.fr).

* *Present address:* INSA de Lyon, Laboratoire des Matériaux Macromoléculaires, Batiment 403, 20 Avenue Albert Einstein, 69621 Villeurbanne Cedex, France.

Journal of Applied Polymer Science, Vol. 79, 2038–2051 (2001)

be produced with low molecular weight and large polydipersity index.

Mainly, two approaches are used industrially to overcome these difficulties. The first one is to lower the viscosity of the medium and facilitate mixing and heat transfer by using either a solvant (solution polymerization) or a dispersing fluid (emulsion and suspension polymerization). The second one is to carry on the polymerization in bulk to low conversion just before the onset of the gel effect and then transfer the viscous mixture in molds where the reaction is slowly finished.

A third approach is to polymerize the MMA in bulk or with a small amount of solvent at a temperature above the glass transition temperature of the polymer (T_g = 114°C). The resultant polymer is obtained in the melt state with a viscosity low enough to allow stirring. In the literature, little information is found on the polymerization of MMA at high temperature probably because experimental problems arise. The polymerization has to be run in a pressurized reactor as the boiling temperature of the monomer is 100°C. However, a few attempts have been made in this direction especially in a twin screw extruder[1–3] and in a tubular reactor.[4–6] Most of the time, the authors used the kinetic constants of the polymerization determined at low temperature to modelize their polymerization at high temperature.

However, Corpart,[7] Clouet,[8] Fleury,[9] and Fenouillot[10,11] in previous works have studied the specific features of the polymerization at high temperature. They have shown that at a temperature above 120°C, the thermal initiation and the initiation reaction by imputities cannot be neglected anymore, and depending on the purification method of the monomer can lead to conversions around 10–20%. Moreover, at these temperatures, the gel effect is strongly attenuated and the classical gel effect models do not predict the experimental data well ; they always overestimate the intensity of the gel effect.

The present work focuses on the polymerization of the MMA at temperatures between 120 and 180°C in a pilot continuous reactor that we describe as "imperfectly mixed." The reaction is carried out with di-*tert*-butyle peroxide (DTBP) as initiator and 1-butanethiol (BSH) as a chain transfer agent. No solvent is used. The steady state behavior of the reactor is modeled based on our earlier study of the kinetic aspects of the reaction.[10,11] The experimental results obtained on the pilot reactor are compared with the predicted values.

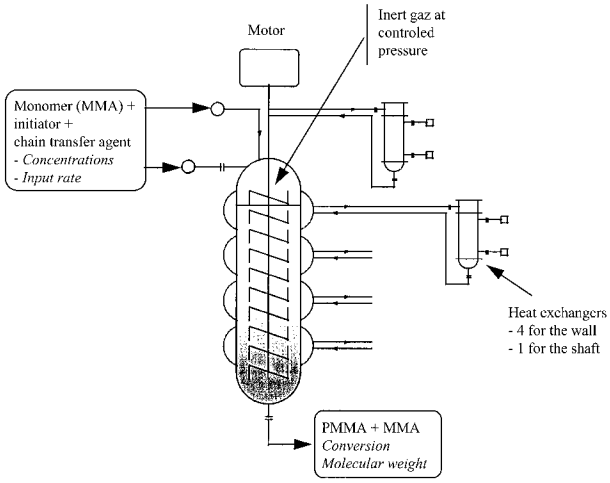

Figure 1 Continuous reactor.

EXPERIMENTAL SYSTEM AND PROCEDURE

The reactor is an agitated vertical vessel with a volume of 20 L (Fig. 1); the mean residence time in the reactor is 3–4 h. The wall of the reactor and the agitator shaft are temperature regulated by a hot oil circulation. Four independent heating zones exist along the reactor and a fifth one for the agitator. The rotation speed of the agitator ranges from 0 to 60 rotations per minute. The reactor is pressurized with an inert gaz and the pressure is regulated at a constant value high enough to avoid boiling of the monomer. The commercial MMA is supplied by Atochem, it is stabilized with 15 ppm of 4-methoxy phenol. The monomer is purified by distillation at low temperature and low pressure of inert gas. The DTBP and the BSH are used as received (99% purity). The monomer and the polymerization additives are preheated and mixed on line through a specially designed static mixer. The reactive mixture is fed at the top of the reactor. At the bottom of the reactor, where the degree of conversion may reach 80%, the solution of polymethylmethacrylate (PMMA) with MMA is transfered to a devolatilization extruder to eliminate the residual monomer. The monomer conversion, X, is calculated by dividing the massic output rate of polymer ($Q_m - Q_{mc}$) by the massic feed rate of the monomer, Q_m. Q_{mc} is the massic flow rate of the condensate.

Table I Kinetic Scheme for the Bulk Polymerization of MMA at High Temperature[a]

Thermal initiation	$2M \xrightarrow{k_{th}} 2R^{\bullet}$
Initiation by the chain transfer agent	$A \xrightarrow{k_{dt}} R^{\bullet}$
Initiation	$I \xrightarrow{k_d} 2R^{\bullet}$
	$R^{\bullet} + M \xrightarrow{k_i} P_1^{\bullet}$
Propagation	$P_n^{\bullet} + M \xrightarrow{k_p} P_{n+1}^{\bullet}$
Depropagation	$P_n^{\bullet} \xrightarrow{k_{dp}} P_{n-1}^{\bullet} + M$
Termination by disproportionation	$P_n^{\bullet} + P_m^{\bullet} \xrightarrow{k_{td}} P_n + P_m$
Termination by combination	$P_n^{\bullet} + P_m^{\bullet} \xrightarrow{k_{tc}} P_{n+m}$
Chain transfer to monomer	$P_n^{\bullet} + M \xrightarrow{k_{trm}} P_n + P_1^{\bullet}$
Chain transfer to the chain transfer agent	$P_n^{\bullet} + A \xrightarrow{k_{trt}} P_n + A^{\bullet}$

[a] k_d: rate constant for the dissociation of the initiator (s^{-1}); k_{dp}: depropagation rate constant (s^{-1}); k_{dt}: apparent rate constant for the initiation by chain transfer agent (s^{-1}); k_p, k_t: rate constant for termination and propagation (L mol^{-1} s^{-1}); k_{tc}, k_{td}: rate constant for termination by combination and disproportionation (L mol^{-1} s^{-1}); k_{th}: rate constant for the thermal initiation (L mol^{-1} s^{-1}); k_{trm}: rate constant for chain transfer to the monomer (L mol^{-1} s^{-1}); k_{trt}: rate constant for chain transfer to the mercaptan (L mol^{-1} s^{-1}).

$$X = \frac{Q_m - Q_{mc}}{Q_m} \tag{1}$$

The reactor is not a perfectly mixed reactor as the agitation speed is moderate and because there is a ratio of 20 between its height and its width. In the first upper portion of the reactor where the monomer is fed, the conversion is very low while it reaches 80% at the bottom of the reactor. A gradient of physical properties, concentration, viscosity, temperature, density, and polymerization rate is established along the reactor. The heat produced by the polymerization reaction varies along the reactor ; it is much higher in the upper part where the polymerization rate is high. On the other hand, in the lower part of the reactor where the polymerization rate is low the heat release from the mechanical work of the agitator may become predominant because of the high viscosity of the medium.

The flow and mixing behavior of the reactor is intermediate between a tubular (plug flow reactor) reactor and a mixed flow reactor. That is what we verified by measuring the residence time distribution of the reactor.

POLYMERIZATION MECHANISM AND KINETICS

The bulk polymerization of MMA is run at elevated temperature (120–180°C) and initiated by DTBP; BSH is used to control the molecular weight. We have detailed the kinetics of this reaction system in previous studies[10,11] showing that some particularities must be taken into account for above T_g polymerization. The monomer used in the batch reactor to establish the kinetics[11] and to run this continuous reactor is distillated with the same procedure, except that in the case of the continuous reactor, the monomer is stored and transported under an inert gas. Since the monomer is not put in contact with air before being pumped into the reactor, the initiating impurity, which we suspected to be oxygen, is absent from our monomer and we decided to eliminate its contribution to the initiation process (Table I).

The rate constants of the reactions are summarized in Table II with the model adopted to account for the attenuation of the gel effect at high temperature. The quasi steady state assumption for polymer radical is not made.

Table II Kinetic Rate Constants Used in the Model

Kinetic Rate Constant for the MMA Polymerization		
$k_p = k_{p0} = 4.92 \times 10^5 \exp(-2191/T)$	(L mol^{-1} s^{-1})	Ref. 16
$k_{dp} = 6.48 \times 10^{11} \exp(-9185/T)$	(s^{-1})	Ref. 16
$k_{t0} = 9.8 \times 10^7 \exp(-353/T)$	(L mol^{-1} s^{-1})	Ref. 16
$k_{tc}/k_{td} = 3.956 \times 10^{-4} \exp(2065/T)$	—	Ref. 16
$k_d = 2.8 \times 10^{14} \exp(-17617/T)$	(s^{-1})	Ref. 17
$f = 1$	—	Ref. 11
$k_{th} = 9.54 \times 10^{-2} \exp(-10900/T)$	(L mol^{-1} s^{-1})	Ref. 11
$k_{dt} = 6.78 \times 10^7 \exp(-15480/T)$	(s^{-1})	Ref. 11
$k_{trm}/k_p = 2.024 \exp(-4006/T)$	—	Ref. 11
$k_{trt} = 8.93 \times 10^6 \exp(-3567/T)$	(L mol^{-1} s^{-1})	Ref. 11
Gel Effect Constitutive Equations		
$\frac{1}{k_t} = \frac{1}{k_{t0}} + \frac{1}{k_{t0}\exp[\beta(X_c - X)]}$		Ref. 11
$\beta = -17.85 + 0.5756T - 0.002519T^2$		
$X_c = 4.289 - 0.05799T + 0.00020422T^2 + 0.11\ \mathrm{Ln}(1000A_0 + 3)$		
Other Parameters Used		
$\varepsilon = -(0.2256 + 4.81 \times 10^{-4}T + 4.1 \times 10^{-4}T^2)$		Ref. 18
$M_m = 100.13$ g mol^{-1}		
$d_m(T) = 0.968 - 1.225 \times 10^{-3} \times T$		Ref. 17

REACTOR MODEL

A tanks in a series model with backflow is proposed to describe the flow and mixing in the pilot reactor (Fig. 2). The parameters of the model are the number of tanks, their volumes, and the backflow rate that may be considered variable or constant from one reactor to the other. However, on the base of some preliminary calculations with a simplified simulation program we have chosen to keep only two parameters. The first reason is that the number of reactors was found to have a determinant effect while the three other parameters had only a second order effect on the residence time distribution of the reactor. The second reason to limit the number of parameters is that the actual reactor is assimilated to the model through a parameter estimation technique, and the adjustment of more than two parameters is quite subjective and questionable.

The parameters of the model are the number of reactors n_{reac} and the volumetric flow rate of recycled material q. The ideal mixed reactors are of equal volume V.

We take into account the density changes of the reacting medium produced by the polymerization reaction and by the temperature variations. As a consequence, the volumetric flow rate varies for each reactor ; it is a function of the conversion and of the temperature in each ideal reactor. The conservation of the massic flow rate allows us to write for the reactor k

$$Q_m(\mathrm{input}) = Q_m(\mathrm{output}) = Q_m \tag{2}$$

$$Q_{k-1}d_{k-1} + qd_{k+1} = (Q_k + q)d_k \tag{3}$$

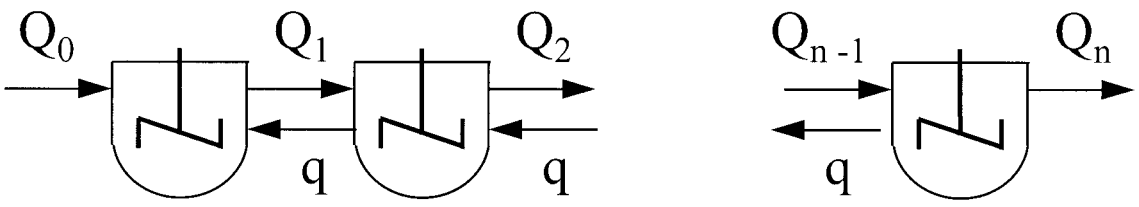

Figure 2 Reactor model.

Q_k is the volumetric flow rate in reactor k, d_k is the density of the solution in reactor k. It is a function of the monomer concentration.

$$d_k = \frac{d_{mk} + \varepsilon_k M_m [M]_k}{1 + \varepsilon_k} \quad (4)$$

$[M]_k$ is the monomer concentration, M_m is the molecular weight of the monomer. d_{mk} is the density of the monomer, ϵ_k is the expansion coefficient in reactor k ; they depend on the temperature in the considered reactor.

At steady state, the mass balance equations for a cascade of continuous stirred tank reactors (CSTR) of constant volume V with a recirculation rate of q takes the following form:

$$Q_{k-1}[M]_{k-1} + q[M]_{k+1} + VR_k^M = (Q_k + q)[M]_k \quad (5)$$

$$Q_{k-1}[I]_{k-1} + q[I]_{k+1} + VR_k^I = (Q_k + q)[I]_k \quad (6)$$

$$Q_{k-1}[A]_{k-1} + q[A]_{k+1} + VR_k^T = (Q_k + q)[A]_k \quad (7)$$

$$Q_{k-1}\lambda_{0k-1} + q\lambda_{0k+1} + VR_k^{\lambda 0} = (Q_k + q)\lambda_{0k} \quad (8)$$

(5)–(8) as well as the flow rate must be written for each reactor; it is a system of $(n_{\text{reac}} \times 5)$ nonlinear equations with $(n_{\text{reac}} \times 5)$ unknowns.

The average molecular weights are determined with the method of moments. We express the balance equations for the 0, 1, and 2 order moments for the living radicals and for the terminated chains:

$$Q_{k-1}\lambda_{1k-1} + q\lambda_{1k+1} + VR_k^{\lambda 1} = (Q_k + q)\lambda_{1k} \quad (9)$$

$$Q_{k-1}\lambda_{2k-1} + q\lambda_{2k+1} + VR_k^{\lambda 2} = (Q_k + q)\lambda_{2k} \quad (10)$$

$$Q_{k-1}\mu_{0k-1} + q\mu_{0k-1} + VR_k^{\mu 0} = (Q_k + q)\mu_{0k} \quad (11)$$

$$Q_{k-1}\mu_{1k-1} + q\mu_{1k+1} + VR_k^{\mu 1} = (Q_k + q)\mu_{1k} \quad (12)$$

$$Q_{k-1}\mu_{2k-1} + q\mu_{2k+1} + VR_k^{\mu 2} = (Q_k + q)\mu_{2k} \quad (13)$$

($\lambda_{0,1,2}$: 0,1,2 moment of the growing radical; $\mu_{0,1,2}$: 0,1,2 moment of the dead polymer chains.) R_k^C is the rate of production or consumption of the chemical specie C in the reactor k. The equations are given in Table III with the expression of the number and weight average molecular weights $\overline{M_n}$ and $\overline{M_w}$ and the polydispersity index (IP).

Table III Balance Equations for the Bulk Polymerization of MMA

$$R_k^M = -(k_p + k_{trm})[M]_k\lambda_{0k} + k_{dp}\lambda_{0k}$$
$$R_k^1 = -k_d[I]_k$$
$$R_k^A = -k_{dt}[A]_k - k_{trt}[A]_k\lambda_{0k}$$
$$R_k^{\lambda 0} = 2fk_d[I]_k + k_{dt}[A]_k + k_{th}[M]_k^2 - k_t\lambda_{0k}$$
$$R_k^{\lambda 1} = 2fk_d[I]_k + k_{dt}[A]_k + k_{th}[M]_k^2 + k_p[M]_k\lambda_{0k} - k_{dp}\lambda_{0k} + (k_{trm}[M]_k + k_{trt}[A]_k)(\lambda_{0k} - \lambda_{1k}) - k_t\lambda_{0k}\lambda_{1k}$$
$$R_k^{\lambda 2} = 2fk_d[I]_k + k_{dt}[A]_k + k_{th}[M]_k^2 + (k_p[M]_k - k_{dp})(2\lambda_{1k} + \lambda_{0k}) + (k_{trm}[M]_k + k_{trt}[T]_k)(\lambda_{0k} - \lambda_{2k}) - k_t\lambda_{0k}\lambda_{2k}$$
$$R_k^{\mu 0} = (k_{td} + 0.5k_{tc})\lambda_{0k}^2 + (k_{trm}[M]_k + k_{trt}[A]_k)\lambda_{0k}$$
$$R_k^{\mu 1} = k_t\lambda_{0k}\lambda_{1k} + (k_{trm}[M]_k + k_{trt}[A]_k)\lambda_{1k}$$
$$R_k^{\mu 2} = k_t\lambda_{0k}\lambda_{2k} + k_{tc}\lambda_{1k}^2 + (k_{trm}[M]_k + k_{trt}[A]_k)\lambda_{1k}$$

Equations for the average molecular weights

$$\overline{M}_{nk} = M_m\frac{\lambda_{0k} + \mu_{0k}}{\lambda_{1k} + \mu_{1k}}$$
$$\overline{M}_{wk} = M_m\frac{\lambda_{2k} + \mu_{2k}}{\lambda_{1k} + \mu_{1k}}$$
$$\text{IP}_k = \frac{(\lambda_{0k} + \mu_{0k})(\lambda_{2k} + \mu_{2k})}{(\lambda_{1k} + \mu_{1k})^2}$$

Notice that the calculation of the moments may be done independently by solving 5 systems of n_{reac} linear equations with n_{reac} unknowns.

The degree of conversion is defined as the ratio between the mass of polymer in the reactor k, mp_k, and the total weight of the solution, $mp_k + mm_k$ (mm: mass of the monomer). The conversion is expressed as a function of the monomer concentration in each reactor:

$$X_k = \frac{mp_k}{mp_k + mm_k} \quad (14)$$

$$X_k = \frac{d_{mk} - M_m[M]_k}{d_{mk} + \varepsilon_k M_m[M]_k} = 1 - \frac{M_m[M]_k}{d_k} \quad (15)$$

Energy Balance

Each reactor is a CSTR with a constant temperature T_k. The energy balance is expressed in the following way for the reactor k:

$$Q_{k-1}d_{k-1}C_p(T_{k-1} - T_k) + qd_{k+1}C_p(T_{k+1} - T_k) + Sp_kU_k(Tp_k - T_k) + Sa_kU_k(Ta_k - T_k) + Spa_kU_k(Ta_k - T_k)Ch - \Delta H_pR_k^MV + V\dot{\gamma}_R^2\eta_k + V\dot{\gamma}_p^2\eta_{pk} = 0 \quad (16)$$

Table IV Correlations Used for the Thermal Exchanges in the Reactor[a]

Calculation of the conductance — Refs. 12, 13

$$\mathrm{Nu}_{\mathrm{int}\,k} = a\,\mathrm{Re}_k^b \mathrm{Pr}_k^{1/3}\left(\frac{\eta_k}{\eta_{pk}}\right)^m$$

$$\mathrm{Nu}_k = \frac{h_{\mathrm{int}\,k} D_r}{\lambda_k}$$

$$\mathrm{Re}_k = \frac{d_k N (D_r - e)^2}{\eta_k}$$

$$\mathrm{Pr}_k = \frac{\eta_k C_p}{\lambda_k}$$

with $a = 1$, $b = 0.5$, $m = 0.18$

Thermal conductivity of the MMA/PMMA solution — Ref. 4

$\lambda = X\lambda_m + (1 - X)\lambda_p$

$$\lambda_m = \frac{19900}{T}\left(\frac{0.9665 - 0.0011(T - 273.15)}{100.12}\right)^{4/3} \mathrm{W\ m^{-1}\ K^{-1}}$$

$\lambda_p \approx 0.165$ W m^{-1} K^{-1}

$C_p = 1672$ J kg^{-1} K^{-1}

[a] a, b, m: Parameters to calculate Nu; Nu: Nusselt number; Pr: Prandtl number; λ, λ_m, λ_p: thermal conductivity of the solution, the monomer, and the polymer.

U_k is the heat transfer coefficient, Sp_k is the exchange area for the wall of the reactor, Sa_k is the exchange area for the shaft of the agitator, Spa_k is the excange area for the blades of the agitator, Ch is a coefficient to calculate the temperature of the blades, η_k and η_{pk} are the viscosity of the solution in the bulk and near the wall.

The heat transfer resistance through the wall of the reactor is neglected, thus the temperature of the wall Tp and of the shaft Ta are considered equal to the temperature of the circulation oil. The temperature of the blades is estimated later.

The heat of polymerization ΔH_p the heat capacity of the solution C_p and the shear rate in the reactor and at the top of the blades, $\dot{\gamma}_R$ and $\dot{\gamma}_p$ are taken constant along the reactor.

Our simplified preliminary calculation and the study of Kim[12] have shown that it was necessary that the heat transfer coefficient is a function of the viscosity of the reacting medium. The heat transfer coefficient U_k varies along the reactor as it depends on the viscosity and on the Reynolds number, Re. To simplify, the conductance in the wall of the reactor and the heat transfer in the regulation oil are neglected. The global heat transfer coefficient is equal to the transfer contribution of the reaction mixture side.

$$U_k = h_{\mathrm{int}\,k} \tag{17}$$

where h_{int} is the heat conductance. The correlation used to calculate the thermal conductance are given in Table IV.

Heat Exchange with the Blades of the Agitator

The geometry of the blades is simplified in order to calculate their average temperature (Fig. 3). The blade is assimilated to a plate with a thickness 2δ and a length l. The temperature along the blade at the position x, $T(x)$, is given by the following relation[14]:

$$\frac{T(x) - T_k}{Ta_k - T_k} = \frac{ch\left[\sqrt{\frac{U_k}{\lambda\delta}}\,1\left(1 - \frac{x}{1}\right)\right]}{ch\left[\sqrt{\frac{U_k}{\lambda\delta}}\,1\right]} = Ch \tag{18}$$

The temperature profile is almost linear because the blades are short and thick. We consider that the average temperature of the blade is equal to

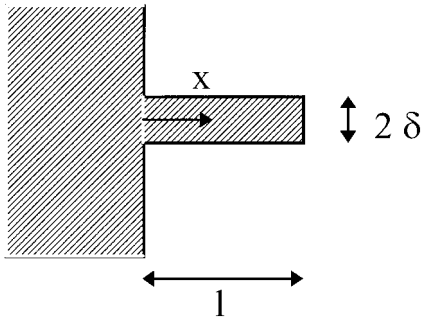

Figure 3 Simplification of the design of the blade used to calculate its average temperature.

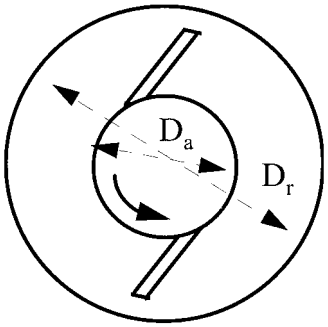

Figure 4 Simplified view of the cross section of the reactor.

the temperature calculated at the position $x = 1/2$. The thermal power exchanged by the blades is

$$U_k Spa_k (Ta_k - T_k) Ch \tag{19}$$

The heat dissipation by shearing the viscous solution has been taken into account in the following way: the mechanical heat dissipation is quite different whether we consider the bulk fluid, between the shaft and the wall, or the fluid near the reactor wall at the top of the blades. The shear rate into the reactor is low ($\approx 4\ s^{-1}$) but it concerns the overall PMMA/MMA solution. On the other hand, the shear rate at the wall surface is high ($300\ s^{-1}$) but is applied to a small volume and during a short period of time, when the blades sweep the wall.

The rheological data, shear rate and viscosity, are necessary to express the energy balance.

To calculate the shear rate in the main volume, the geometry of the reactor is approximated to two coaxial cylinders, the inner cylinder is rotating and does not have blades (equivalent to a Couette flow). This calculation underestimates the shear rate in the reactor because the blades create a more complex flow pattern than in a Couette geometry (Fig. 4).

$$\dot{\gamma}_r = \frac{4\pi N D_r}{D_r^2 - D_a^2} \tag{20}$$

The shear rate at the wall surface may be expressed by eq. (21) where the geometry is approximated to a plane flow since the gap between the wall of the reactor and the top of the blade is small compared to the diameter of the reactor.

$$\dot{\gamma}_p = \frac{\pi N (D_r - 2e)}{e} \tag{21}$$

D_a and D_r are the diameter of the shaft and the diameter of the reactor. e is the gap between the blade and the wall.

The viscosity of the MMA/PMMA solution is a function of the monomer concentration, the molecular weight of the polymer, the temperature and the shear rate. Stuber[15] has proposed an empirical expression to predict the non-Newtonian viscosity as a function of these parameters.

$$\eta = f(X, \overline{M}_w, T, \dot{\gamma}) \tag{22}$$

The Elllis model allows to calculate the non-Newtonian viscosity of concentrated solutions.

$$\eta(\dot{\gamma}) = \frac{\eta_0}{1 + me\,\dot{\gamma}^{1-n}} \tag{23}$$

where n is the pseudoplasticity index, me is the Ellis constant. The η_0 is the viscosity at zero shear rate, it is calculated with an empirical expression (Table V).

Simulation Program

The kinetic, flow, and thermal aspects of the problem have been integrated in a simulation program that calculates the behavior of the continuous reactor at steady state. First, a calculation is made with simplified expressions of the reaction rates and with the volume contraction and backflow rate taken equal to 0. This preliminary run of the program provides an approximate solution to initiate the resolution of the complete system of nonlinear equations by the Newton-Raphson method.

Starting from the experimental operating conditions of the reactor, the program gives access to data that we may compare with the experimental one (Fig. 5). The only remaining task is to determine the parameters of the reactor model n_{reac} and q. This is achieved by comparing the experimental residence time distribution data collected on the reactor, the measured monomer conversion and average molecular weight of the polymer with their corresponding calculated data. For this purpose, we have run five experiments on the continuous reactor with a variable agitator speed. The

Table V Correlations Used to Calculate the Non-Newtonian Viscosity of the MMA/PMMA Solution[a]

Newtonian viscosity Ref. 15

$$\eta_0(X, \bar{M}_w, T) = \frac{F\xi}{10}$$

$$F = K[1 + a_1(100X\bar{M}_w)^{0.5} + a_2(100X\bar{M}_w)^{3.4}]$$

$$\xi = \exp\left[(b_0 + b_1 100X + b_2 100X^2)\left(\frac{1}{T} - \frac{1}{T_{\text{ref}}}\right) + b_3 100X^3\right]$$

Non-Newtonian viscosity Ref. 15

$$\eta(\dot{\gamma}) = \frac{\eta_0}{1 + me\dot{\gamma}^{1-n}}$$

$$n(X, \bar{M}_w, T) = \exp\left(\frac{-13.8155\bar{M}_w^{0.5}(100X)^4}{T}\right)$$

$$me(X, \bar{M}_w, T) = \exp\left(\frac{1.406.10^6\bar{M}_w^{0.5}(100X)^4}{T}\right)$$

Parameters: $K = 2.16 \times 10^{-3}$, $a_1 = 1.25 \times 10^{-1}$, $a_2 = 3.75 \times 10^{-11}$, $b_0 = 6 \times 10^2$, $b_1 = 8 \times 10^1$, $b_2 = 1$, $b_3 = 1.2 \times 10^{-5}$

$T_{\text{ref}} = 465.15$ K

[a] ξ, a_1, a_2, b_0, b_1, b_2, b_3 F: Parameters to calculate the viscosity; T_{ref}: reference temperature for the calculation of the viscosity; n: pseudoplasticity index.

residence time distribution (RTD) is determined as explained in the next section.

RESULTS AND DISCUSSION

Experimental Determination of the RTD

Toluene is used as the tracer, this choice is probably not the best as toluene may not be representative of the flow of the polymer into the reactor. However, toluene is a small molecule soluble in PMMA at high temperature like MMA is, and we may expect that the flow and diffusion characteristics of the toluene are not so different from those of the monomer.

A small quantity of the tracer is introduced in the reactor at time $t = 0$. As the toluene is a volatile liquid, it is devolatilized with the residual monomer in the extruder placed at the outlet of the reactor. The condensate, a mixture of MMA with a small amount of toluene is then analyzed by infrared spectroscopy to determine the concentration of the tracer in the condensate. The residence time distribution is given by

$$E(t) = \frac{c(t)Q_c}{m_0} \tag{24}$$

where $c(t)$ is the tracer concentration in the condensate, Q_c is the volumetric flow rate of the condensate, m_0 is the calculated mass of tracer injected. m_0 is calculated by integrating the concentration variation. Some tracer, less than 5%, was lost during the experiment.

$$m_0 = \int_0^\infty c(t)Q_c\, dt \tag{25}$$

The experimental conditions of the determination of the RTD are summarized in Table VI as well as the conversion and number average molecular weight obtained. N is the rotation speed of the agitator, T_c is the regulation temperature of the wall and agitator shaft, T_0 is the preheating temperature of the monomer, and I_0 and A_0 are the concentrations of DTBP and BSH, respectively.

Figures 6 shows the measured RTD for each conditions.

For this "imperfectly mixed" reactor, the broadness of the residence time distribution depends on the agitation speed. When the rotation speed of the agitator increases, the reactor tends to behave like a continuous stirred tank reactor (CSTR). At the opposite, when the agitator speed is low the reactor tends to a plug flow reactor. For an agitator speed equal to 0 rpm, the flow in the reactor

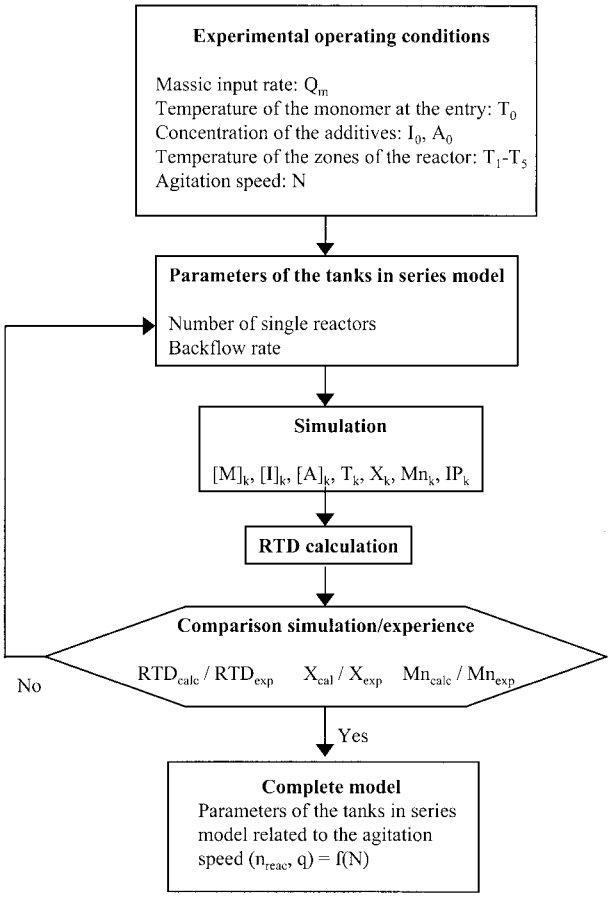

Figure 5 Schematic representation of the simulation program.

will tend to a Poiseuille flow in an annular gap (if we neglect the effect of the agitator blades). The mixing effectiveness is a function of the relative importance of the rotation speed of the agitator compared to the axial displacement speed of the reactive mixture.

These results allow us to relate the parameters of the tanks in a series model to the intensity of the agitation of the actual reactor. When the agitation speed increases the number of reactors of the model decreases and the recycle flow rate increases.

The simulation program is used to determine the relation between n_{reac}, q, and the rotation speed of the agitator (Fig. 7). The calculated and experimental RTDs are represented in Figure 6.

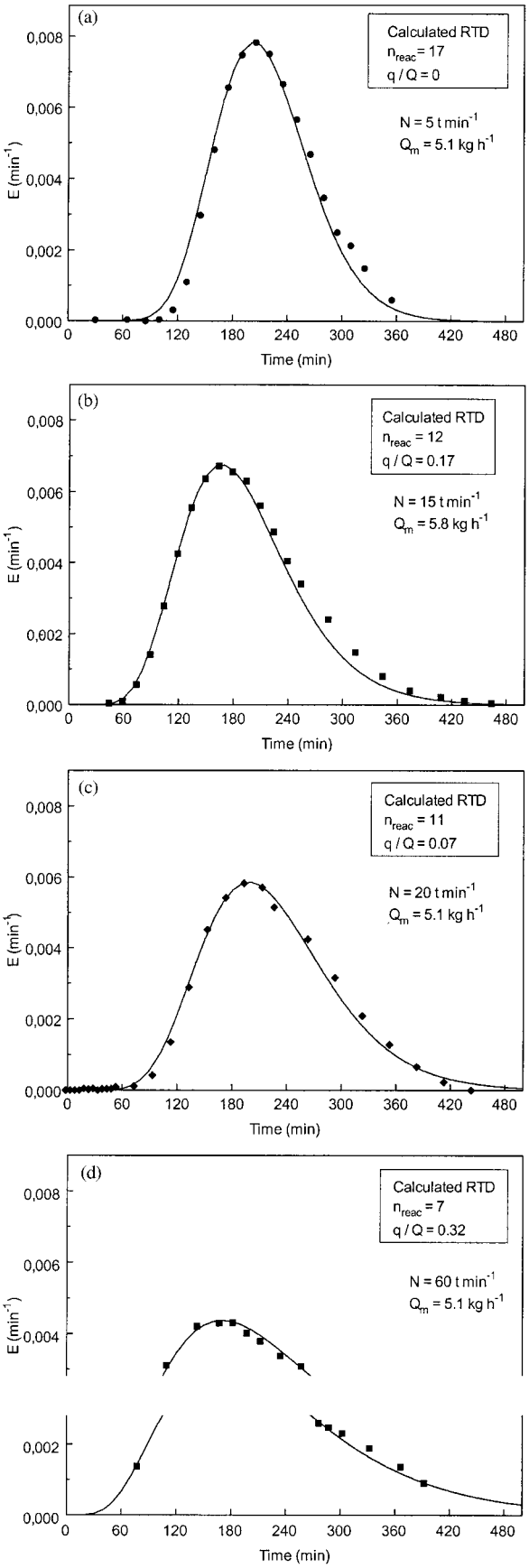

Figure 6 Calculated (line) and experimental (symbols) residence time distribution for different agitator speed. 5, 15, 20 and 60 rotation per minutes.

Table VI Operating Conditions of the Reactor for the RTD Experiments

	Operating Conditions						Experimental and Calculated Results					
Ref.	N (min^{-1})	T_c (°C)	T_0 (°C)	Q_m ($kg\ h^{-1}$)	$[I]_0$ (10^{-3} mol L^{-1})	$[A]_0$ (10^{-3} mol L^{-1})	X_{exp} (%)	X_{calc} (%)	$\overline{M}_n^{exp}$ ($g\ mol^{-1}$)	$\overline{M}_n^{calc}$ ($g\ mol^{-1}$)	IP_{exp}	IP_{calc}
108c[a]	0	150	120	5.1	6.7	10.8	53–69	—	71100	—	2.3	—
108b	5	150	113	5.1	6.7	10.8	53–56	55	68500	63440	2.4	2.08
109b	15	150	120	5.8	5.9	9.7	65	69	79000	76300	2.25	2.02
108a	20	150	113	5.1	6.7	10.8	79	77	77500	70800	2.2	2.02
108d[b]	60	150	122	5.1	6.7	10.8	83	84	78900	71400	2.2	2.01

[a] Operating condition not stabilized.
[b] Short operating condition (8.5 h).

Table VII Comparison of the Measured and Simulated Monomer Conversion and Molecular Weight Data

	Operating Conditions						Experimental and Calculated Results					
Ref.	N (min^{-1})	T_c (°C)	T_0 (°C)	Q_m ($kg\ h^{-1}$)	$[I]_0$ (10^{-3} mol L^{-1})	$[A]_0$ (10^{-3} mol L^{-1})	X_{exp} (%)	X_{calc} (%)	$\overline{M}_n^{exp}$ ($g\ mol^{-1}$)	$\overline{M}_n^{calc}$ ($g\ mol^{-1}$)	IP_{exp}	IP_{calc}
104d	15	150	138	5.6	9	8.55	61	73.1	82000	78100	2.17	2.04
104f	—	147	—	—	—	—	67.5	76.4	87000	79400	2.22	2.04
104e	—	145	—	—	—	—	72.5–80	78.6	83000	80100	2.44	2.04
104g	—	147	134	6.95	—	—	60	71.6	93000	78200	2.21	2.05
105b	—	150	136	5.4	13.5	8	60.5	73.6	64000	75400	2.68	2.14
105g	—	145	120	7.7	7.7	7.3	63		72000		2.43	
105h	—	148	—	—	—	—	61	65.6		87500		2.06
105i	—	144e–148a	—	—	—	—	66.5	68	93000	88900	2.26	2.06

Table VIII Comparison of the Measured and Simulated Monomer Conversion and Molecular Weight Data

	Operating Conditions						Experimental and Calculated Results					
Ref.	N (min^{-1})	T_c (°C)	T_0 (°C)	Q_m (kg h^{-1})	$[I]_0$ (10^{-3} mol L^{-1})	$[A]_0$ (10^{-3} mol L^{-1})	X_{exp} (%)	X_{calc} (%)	$\overline{M}_n^{exp}$ (g mol^{-1})	$\overline{M}_n^{calc}$ (g mol^{-1})	IP_{exp}	IP_{calc}
204a	20	140/150/160/160/160	120	5.6	7.8	22	76	76.3	31100	38800	2.9	2.01
205a	20	140/150/160/160/160	120	6	7	17.4	62	72.5	35300	47500	2.8	2.01
205b	—	—	—	5.5	7.6	19	68	75.9	33000	44270	3	2.01
205c	—	135/150/160/180/160	—	—	—	—	77.5	76.1	38600	44350	2.65	2.02

Table IX Comparison of the Measured and Simulated Monomer Conversion and Molecular Weight Data

	Operating Conditions						Experimental and Calculated Results					
Ref.	N (min^{-1})	T_c (°C)	T_0 (°C)	Q_m (kg h^{-1})	$[I]_0$ (10^{-3} mol L^{-1})	$[A]_0$ (10^{-3} mol L^{-1})	X_{exp} (%)	X_{calc} (%)	$\overline{M}_n^{exp}$ (g mol^{-1})	$\overline{M}_n^{calc}$ (g mol^{-1})	IP_{exp}	IP_{calc}
203c	20	140/150/160/180/160	120	5.6	6.75	12.75	65	69.5	60000	60400	2.1	2.01
203d	—	—	—	—	—	13.55	64	69.7	51000	56600	2.5	2.01
203e	—		—	—	—	17	70	70.1	43600	48000	2.6	2.01
203h	—	—	—	5.7	10	25	81	75.3	30300	33600	3.1	2.01
203f	—	—	—	5.85	13.4	33.7	75–80	81	22500	25680	3.3	2.01

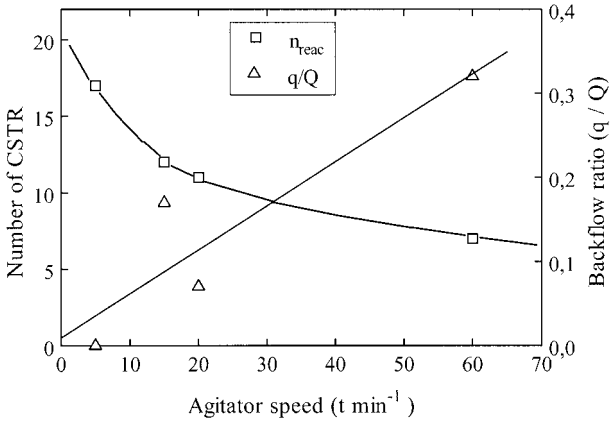

Figure 7 Relation between the parameters of the reactor model (number of reactor and backflow rate) and the speed of the agitation.

The number of CSTR has the most significant effect on the shape of the RTD curves and on the monomer conversion. The backflow rate q has less influence.

Simulation of the Experiments

The experimental data collected on the reactor are the following:

— final degree of conversion ($X = Q_{mp}/Q_m$);
— final average molecular weights measured by size exclusion chromatography (SEC) with a PMMA calibration;
— temperature of the reacting medium at four places along the reactor.

The simulation program gives access to the following data for each CSTR: concentration of the chemical species, monomer conversion, average molecular weights of the PMMA, temperature, heat exchange coefficcient, viscosity.

The temperature of the reactor has a determinant effect on the conversion obtained (Table VII, compare experiments 104d–f). When the temperature decreases the gel effect is more pronounced and the initiator is more effective as it is less burnt out, the result is a higher conversion. This trend was also observed in the batch reactor.[10,11] These operating conditions are not comfortable because at low temperature and consequently high conversion, the viscosity of the medium increases and it becomes difficult to maintain the agitation because of the limited torque of the motor. The simulation is not very performant to predict the extent of conversion variation produced by the temperature. It predicts an elevation of conversion of 5.5% instead of the 10–15 % actually observed.

The increase in conversion produced by a decrease of the temperature may be compensated by a higher input rate. Compare in Table VII the experiments 104e with 104g and 105b with 105g. The effect of the temperature, input rate, and concentration of the feed mixture is also clearly illustrated when one compares the experiments 205a–c (Table VIII). In this case also the simulation does not predict the same extent of variation than observed.

Another important operating parameter is the agitator speed. The monomer conversion increases of 30% when the agitator speed is increased from 5 to 60 rpm (Table VI).

The molecular weight of the polymer produced depends mainly on the concentration of the chain transfer agent. No clear dependence of the molecular weight on the other operating parameters was detected. The agreement between the calculated and measured molecular weight is correct but tends to degrade when the molecular weight decreases (Fig. 8). The polydispersity index is allways slightly underestimated (see result tables).

For some of the experiments we had four thermocouples measuring the temperature directly in the MMA/PMMA solution. They were placed along the reactor and it is interesting to compare the measurements with the calculation (Fig. 9). The agreement is not always as good as in the case of Figure 9b, an error of 4°C is made for experiment 205 a.

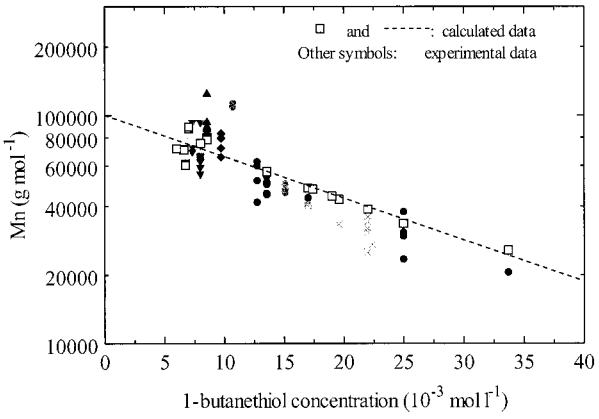

Figure 8 Calculated number average molecular weight (line and □) and experimental data (other symbols) as a function of the concentration of chain transfer agent. All experiments are reported.

One interesting objective of the simulation is to predict the effect of a modification of the design of the reactor, for instance the design of the agitator shaft. The current shaft is temperature regulated with circulating oil, and of course it would be less complex and expensive to build a simple shaft without oil circulation. The question is to determine wether the temperature would stay to a reasonable value. We select a standard operating condition and we impose that the shaft is not temperature regulated anymore by considering that its behavior is adiabatic. In the calculations it is equivalent to say that its heat exchange area is equal to zero. The temperature profiles in the reactor are represented for an adiabatic and a temperature regulated shaft (Fig. 10). In the upper part of the reactor where the polymerization rate is high, the temperature raises of 10°C with the adiabatic shaft. The consequence is a lower final conversion caused by the burn out of the initiator. This calculation shows that it is possible to operate with a simpler agitator but the operating zone of the reactor would be reduced.

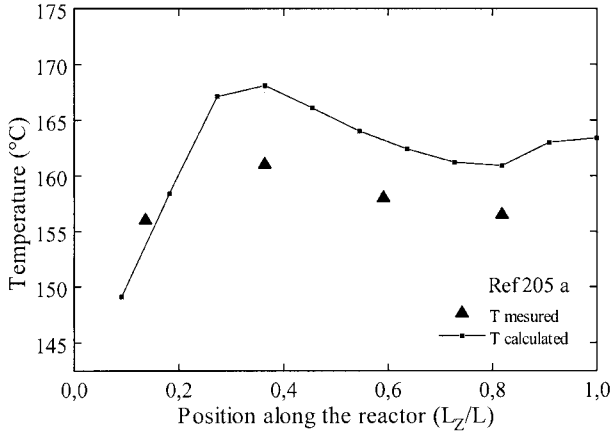

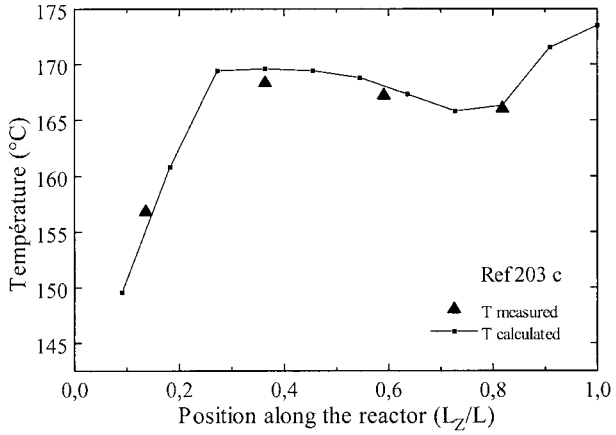

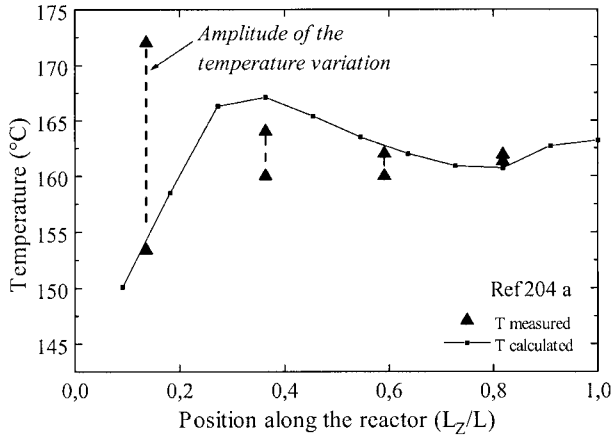

Figure 9 Temperature measured in the reacting mixture as a function of the position in the reactor compared to the calculated one. The experiments references are 205 a, 203 c and 204 a.

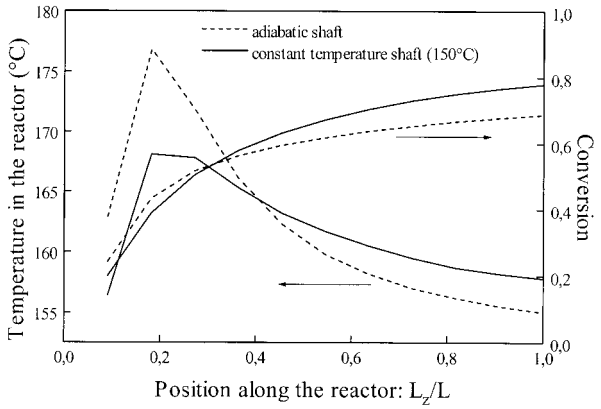

Figure 10 Simulation of the effect of a modification of the shaft design on the behavior of the reactor. The operating parameters are: T_c = 150°C, T_0 = 120°C, $[I]_0$ = 7×10^{-4} mol l^{-1}, $[A]_0$ = 12×10^{-3} mol l^{-1}, N = 20 t min^{-1}, Q_m = 5 kg h^{-1}.

Finally, it is to be noticed that for some of the operating conditions the reactor exhibits an unstable oscillatory behavior. The amplitude of the oscillation is large in the upper part of the reactor and is strongly attenuated as the mixture progresses along the reactor. This behavior is illustrated in Figures 9c and 11. The temperature of the reaction mixture oscillates of about 15°C at the top of the reactor and the residual oscillation is less than 1°C at the bottom.

Some authors[12,19] have studied the dynamic behavior of CSTR, and predicted such instabilities with a much larger amplitude of 30–50°C, possibly because their polymerization temperature was low (70°C) and the gel effect stronger.

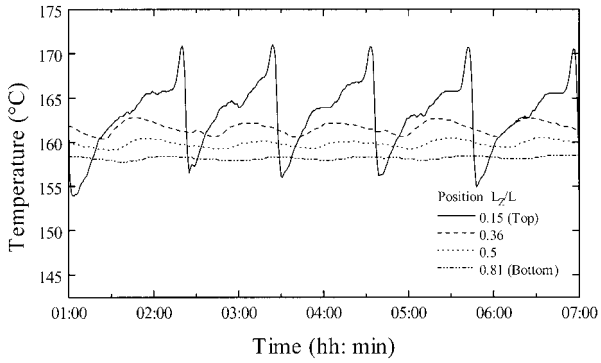

Figure 11 Oscillatory behavior of the reactor. The temperature of the reacting medium measured at four positions in the reactor is plotted as a function of time. Operating conditions reference 204 a: T_c = 140–150–160°C, T_0 = 120°C, Q_m = 5.6 kg h^{-1}, $[I]_0 = 7.8 \times 10^{-4}$ mol l^{-1}, $[A]_0 = 22 \times 10^{-3}$ mol l^{-1}, N = 20 t min^{-1}.

CONCLUSION

The steady state behavior of a pilot continuous reactor has been investigated for the bulk polymerization of MMA at high temperature. The experimental study has shown that monomer conversion up to 80% could be obtained in this reactor. The conversion is influenced mostly by the temperature and the agitator speed of the reactor. For the tested operating conditions, the number average molecular weight of the polymer produced ranges from less than 30,000 to 95,000 g mol^{-1} with a polydispersity index between 2.1 and 3. Since the concentration of the chain transfer agent controls the molecular weight, the other operating parameters like temperature and flow rate play only a secondary role in the obtention of the molecular weight. The main limitation to increase the conversion and the molecular weight comes from the maximum torque accepted by the agitator shaft and blades.

A simulation program was built to calculate the steady state behavior of the actual reactor. The pilot reactor may not be approximated to an ideal reactor because its hight to width ratio is equal to 20. In addition, the agitation speed is low and the reactive mixture very viscous. The RTD measurements have allowed to identify the actual reactor to a tanks-in series model with backflow, much more representative of the "imperfectly mixed" nature of our reactor. The calculated data obtained with the computer program (conversion, molecular weight) appeared to be less sensitive to the changes in operating conditions than the actual reactor. However, the simulation is a powerful tool to predict the effect of design modifications of the reactor. Finally, a dynamic analysis would be necessary to understand why an oscillatory behavior is sometimes observed.

REFERENCES

1. Stuber, N. P.; Tirrel, M. Polym Proc Eng 1985, 3 (1 & 2), 71–83.
2. Ganzeveld, K. J. Doctoral thesis, University of Groningen, 1992.
3. Dey, S. K.; Biesenberger, J. A. ANTEC 1987, 133.
4. Baillagou, P. E.; Soong, D. S. Polym Eng Sci 1985, 25(4), 212–231.
5. Baillagou, P. E.; Soong, D. S. Polym Eng Sci 1985, 25(4), 232–244.
6. Fleury, P. A.; Meyer, T.; Renken, A. Chem Eng Sci 1992, 47(9), 2597–2602.
7. Corpart, P. Doctoral thesis, Université Louis Pasteur de Strasbourg, 1990.
8. Clouet, G.; Chaumont, P.; Corpart, P. J Polym Sci Part A Polym Chem 1993, 31, 2815.
9. Fleury, P. A. Doctoral Thesis, Université de Lausanne (EPFL), 1993.
10. Fenouillot, F.; Terrisse, J.; Rimlinger, T. Intl Polym Proc 1998, 8(2), 154.
11. Fenouillot, F.; Terrisse, J.; Rimlinger, T. J Appl Polym Sci 1999, 72, 1589–1599.
12. Kim, K. J.; Choi, K. Y. Polym Eng Sci 199232, 494–505.
13. Rase, H. F. Chemical Reactor Design for Process Plants; John Wiley & Sons: New York, 1977; Vol 1.
14. Leontiev, A. Théorie des échanges de chaleur et de masse; Editions Mir, 1985.
15. Stuber, N. P. Doctoral thesis, University of Minnesota, 1986.
16. Chiu, W. Y.; Carratt, G. M.; Soong, D. S. Macromolecules 1983, 16, 348.
17. Brandup, J.; Immergut, E. H. Polymer Handbook; John Wiley & Sons: New York, 1975.
18. Stickler, M. Makromol Chem 1983, 184, 2563.
19. Teymour, F.; Ray, W. H. Chem Eng Sci 1989, 44, 9, 1967–1982.